MASTER´S THESIS

Quantifying the influence of pruning treatments on olive tree architecture using UAV technology, 3D models and object-based image analysis

Master´s Degree in Geomatics, Remote Sensing and Spatial Models applied to Forest Management

Course 2015/2016

Student: Francisco Manuel Jiménez Brenes

Directors: Dr. José Manuel Peña Barragán
Dr. Alfonso García-Ferrer Porras

Cordoba, October 2016

Master´s Thesis

Quantifying the influence of pruning treatments on olive tree architecture using UAV technology, 3D models and object-based image analysis

Master´s Degree in Geomatics, Remote Sensing and Spatial Models applied to Forest Management

Course 2015/2016

Director:

Firmado digitalmente por José M
Fecha: 2016.10.10 14:04:05 +02'00'

Dr. José Manuel Peña Barragán

Director:

NOMBRE GARCIA FERRER PORRAS ALFONSO - NIF 30417127H

Firmado digitalmente por NOMBRE GARCIA FERRER PORRAS ALFONSO - NIF 30417127H
Nombre de reconocimiento (DN): c=ES, o=FNMT, ou=FNMT Clase 2 CA, ou=500780156, cn=NOMBRE GARCIA FERRER PORRAS ALFONSO - NIF 30417127H
Fecha: 2016.10.10 13:57:43 +02'00'

Dr. Alfonso García-Ferrer Porras

Author:

Firmado digitalmente por NOMBRE JIMENEZ BRENES FRANCISCO MANUEL - NIF 48981503J
Fecha: 2016.10.10 14:04:45 +02'00'

Francisco Manuel Jiménez Brenes

CONTENT

Abstract **1**

1. Introduction **2**

2. Materials and Methods **5**

2.1. Study area and description of the pruning treatments 5

2.2. Multi-temporal UAV flights and image acquisition 6

2.3. Generation of the UAV image-based products: the 3D point cloud, the Digital Surface Model (DSM) and the image ortho-mosaic 9

2.4. Computing the olive tree geometric features by object-based image analysis (OBIA) 11

2.5. Data analysis and validation 14

3. Results **15**

3.1. Evaluation of the procedure 15

3.2. Influence of the pruning treatment in the tree geometry 16

3.3. Multi-temporal variation of the tree geometry as affected by the pruning treatment 22

4. Discussion **28**

5. Conclusions **32**

6. Acknowledgments **33**

7. References **33**

Abstract

Olive tree pruning is one of the most important crop management tasks and becomes a costly practice with implications in harvesting, nutrition, pest and disease control, or irrigation strategies. The type and intensity of the pruning strategy modifies the tree crown with a different degree of severity, which notably affects tree physiology, olive growing and fruit quality. In this research, it is reported a procedure based in combining UAV technology and advanced OBIA methodology to reach high-throughput quantification and detailed three-dimensional (3D) monitoring of an olive tree plantation in which their trees have been affected by three different pruning treatments (traditional, adapted and mechanized). Three flights were performed over the olive plot (before pruning, one month after pruning and almost a year after pruning) and interesting differences could be discerned among all analyzed variables for every tree: crown projected area, tree height and crown volume. The OBIA algorithm used achieved high percentages of trees correctly defined in all analyzed dates except in the areas where DSM had been generated with a lower accuracy. It was checked the olive trees located under adapted pruning, the treatment where a large amount of foliage was removed, showed the highest foliage extraction after pruning followed by trees under traditional pruning, but also experienced higher growths than the other ones, being quantified this response vegetative almost a year after pruning. The trees corresponding to the mechanized pruning treatment kept a more constant vegetative growth along the research. Due to there is almost no information about the assessment of different pruning treatments on the olive tree crown by UAV technology, this research opens the doors towards a wide study area in the agronomical sector, with interesting applications in precision oliviculture although also possibly in other woody crops.

1. Introduction

The olive tree (*Olea europaea* L.) is one of the most important crops in the Mediterranean basin, where it presents a great economic, social and cultural importance. The cultivated area in Spain totaled 2.6 million hectares in 2015, registering an annual production of almost 4.5 million tonnes (MAGRAMA, 2015). Spain is the world's largest producer of olive oil, and the province of Jaen contains the country's highest concentration of olive groves, producing more oil than Italy, the second largest producer country (Huete and Marmolejo 2016).

Many factors, some of them regarding orchard management tasks, regulate olive production and, subsequently, impact crop viability. Among the main tasks, tree pruning remains as a costly practice with implications in harvesting (Ferguson et al. 2012), nutrition, pest and disease control, or irrigation strategies (Connor et al. 2014). The type and intensity of the pruning strategy modifies the tree crown with a different degree of severity, which notably affects tree physiology and, consequently, olive growing and fruit quality (Castillo-Ruiz et al. 2016; Villalobos et al. 2006).

Investigations on tree pruning usually involve characterization of tree architecture and measurement of crown geometric features. However, obtaining these data is complex mainly due to the relatively small three-dimensional (3D) space of the tree and the irregular geometry of the tree crown (Zheng and Moskal 2009). The conventional method consists on using a ruler to measure the main dimensions of the tree and, next, estimating the crown volume by applying equations that treat the trees as regular polygons or by applying empiric models (West 2009). Obviously, this task is very tedious, needs of an intensive field work and usually generates inconsistent results. Nevertheless, recent advances in new sensors and geo-spatial technologies are offering a cost-effective alternative to hands-on measurement tasks. Rosell and Sanz (2012) described the following techniques: ultrasound, digital photographic techniques, light sensors, high-resolution radar images, high-resolution X-ray computed tomography, stereo vision and LiDAR sensors. These authors claimed LiDAR laser scanners and stereo vision systems to probably be the most promising and complementary techniques for achieving 3D data of the crop canopy. However, these techniques pose some limitations in real crop scenarios. On the one hand, the terrestrial devices can be very precise to measure tree architecture (Fernández-Sarría et al. 2013; Rovira-Más et al. 2008), but they are inefficient in large spatial extents and are difficult to use in rugged areas. On the other hand, remote-sensed data collected with piloted aircrafts and satellites do not often fulfill the technical requirements (e.g., sufficient spatial resolution or number of stereoscopic pairs) needed to detect the 3D characteristics of agricultural trees in most cases (Rosell and Sanz 2012).

Recently, the drones or Unmanned Aerial Vehicles (UAV) have become an efficient tool for continuously collecting information in agriculture. In several investigations (Herwitz et al. 2004; Xiang and Tian 2011; Zhang and Kovacs 2012) have been demonstrated the advantages of the UAVs in comparison to the technologies described above due mainly to its low cost and greater flexibility in flight scheduling (Torres-Sánchez et al. 2014). In addition, thanks to the UAV can fly at very low altitudes, they offer us high spatial resolution images, which permit the generation of the Digital Surface Model (DSM) using automatic photo-reconstruction methods that are based on the "Structure from Motion" approach for 3D reconstruction. As a consequence, recent investigations have focused on the generation of DSM with UAVs and its interpretation over agricultural areas (Bendig et al. 2014; Díaz-Varela et al. 2015; Zarco-Tejada et al. 2014).

Nevertheless, in order to get all the advantages of this technology it is necessary the application of a robust and automatic image analysis procedures capable of retrieving useful information from the images (Torres-Sánchez et al. 2015; Xu et al. 2015). OBIA, object-based image analysis, is a wide array of techniques through which we can get a high level of automation and adaptability. OBIA improves some limitations of pixel-based methods by grouping adjacent pixels with homogenous spectral values after a segmentation process and by using the created "objects" as the basic elements of analysis (Blaschke et al. 2014). Next, OBIA combines spectral, topological, and contextual information of these objects to address complicated classification issues. This technique has been successfully applied in UAV images both in agriculture (Díaz-Varela et al. 2014; Peña et al. 2013), grassland (Laliberte and Rango 2011) and urban (Qin 2014) scenarios.

In this research, it is reported a procedure for a high-throughput and detailed 3D monitoring of agricultural tree plantations by combining UAV technology and advanced OBIA methodology. After the DSM generation with UAV images, this procedure automatically classifies every tree in the field and computes its position, canopy projected area, tree height and crown volume. This study was focused in the geometrical characterization of each tree of an olive plantation in conventional single-tree by UAV technology, with a low-cost visible-light (RGB) camera onboard. In this plantation, three different pruning treatments were performed and, therefore, three UAV flights were made in several times: 1) before pruning, 2) after pruning and 3) one year after pruning. The specific objectives of this research were classified in three issues:

1) Technological objectives: evaluating the capacity of the image-based UAV technology to create 3D models of an olive plantation with different degree of pruning severity.

2) Methodological objectives: developing and applying an original OBIA algorithm for 3D monitoring of the olive plantation with capacity for automatic computing of the olive tree geometrical features (area, height, volume).

3) Agronomical objectives: studying multi-temporal changes of the olive tree data as affected by the pruning treatment and interpretation of the results. Thus, it was possible to obtain an evaluation of the influence of these treatments on tree crown and getting the growth for each tree.

Alternatively, the study of the tree architecture can also offer valuable information to design site-specific crop management strategies in the context of precision oliviculture, which allows optimizing the application of fertilizer, pesticides, irrigation, etc., with the consequent economic and environmental benefits.

2. Materials and Methods

2.1. Study area and description of the pruning treatments

This research was performed in a private 20-year-old olive plantation, called Calancha and located in Villacarrillo, province of Jaen (southern Spain, central coordinates 38.108N, 3.161W, datum WGS84). A rectangular field of approximately 3 hectares and 13% of average slope was selected for the experiment (Figure 1). This field was composed by 648 olive trees of the Arbequina variety, distributed in 27 trees along and 24 across the field, and with an intensive single-tree pattern of 8x4 m tree spacing.

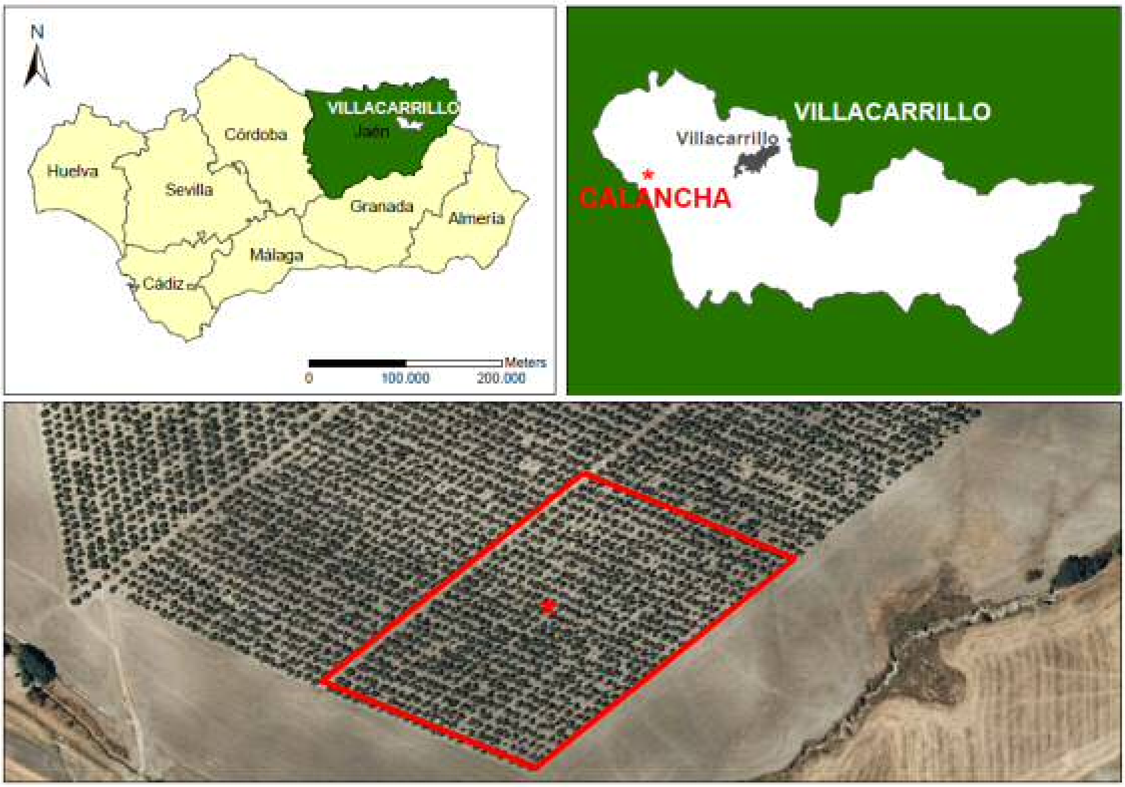

Figure 1. Location of the olive plantation used in this research (up) and aerial view of the experimental plot (down).

The experimental field was divided in three sub-plots of 9x24 trees each one, where traditional, adapted and mechanized pruning treatments were separately performed in March 4th and 5th, 2015 (Figure 2). In the traditional pruning, the highest branches, the crossed ones, as well as those branches below the base of the canopy, established at 60 centimeters over the soil, were pruned. In the adapted pruning, the inner branches were totally removed, plus the crossed and low branches like the previous treatment. Thus, a large number of trees under this treatment presented a big gap in the crown central part. Finally, in the mechanized pruning, a tractor with opposite mechanical cut those branches from 3.5 to 4 meters height at a 30º angle. This tractor also removed the branches located to less than 70 centimeters over the field surface with a horizontal mechanical cut. This last pruning strategy was designed as part of the *Mecaolivar* project, supervised by researchers of the University of Cordoba and the Institute of Agricultural Research and Training (IFAPA, Córdoba), that aimed to study the efficiency of different olive harvest mechanical systems (Mecaolivar 2014).

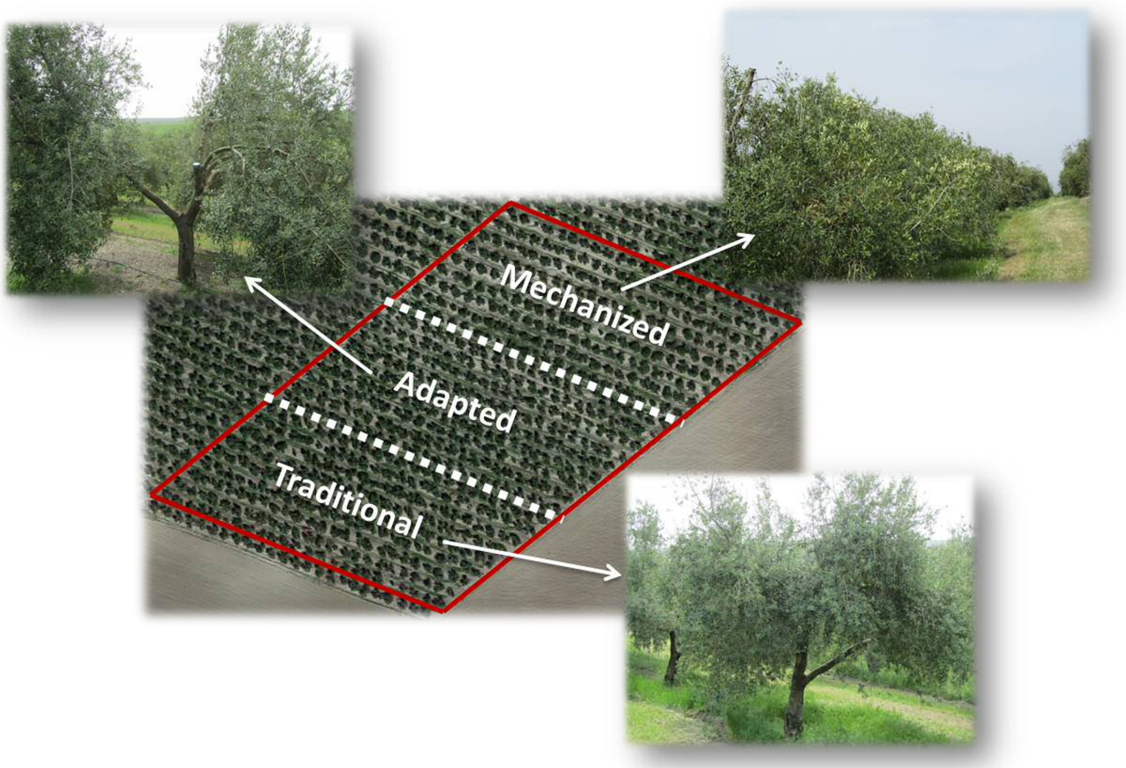

Figure 2. Description of the three pruning treatments performed in the experimental olive field.

2.2. Multi-temporal UAV flights and image acquisition

This research was focused in a multi-temporal analysis of the olive plantation, aiming to quantify the changes of a large number of olive trees due to the application of different pruning treatments. For that, remote images of the experimental field were acquired with UAV flights carried out in three different dates: 1) before pruning (December 9th, 2014), 2) short time after pruning (April 14th, 2015), and 3) almost a year after pruning (February 1th, 2016).

The flight equipment was a quadrocopter UAV with vertical take-off and landing (VTOL), model MD4-1000 (microdrones GmbH, Siegen, Germany), and a still point-and-shoot camera, model Olympus PEN E-PM1 (Olympus Corporation, Tokyo, Japan) (Figure 3). This UAV model has four brushless motors powered by a battery and it can be manually operated by radio control or it could fly autonomously with the aid of its Global Position System (GPS) receiver and its waypoint navigation system. In comparison to the fixed-wing UAVs, one of the main advantages of the VTOL system is its capacity to operate in steep areas without a wide landing zone. The camera onboard the UAV takes 12.2 megapixel format (4,032 x 3,024 pixels) images in true colour (Red, R; Green, G; and Blue, B, bands) with 8-bit radiometric resolution, which are stored in a secure digital SD-card. It uses a 14–42 mm zoom lens, although it was fixed at 14 mm focal length for this work. The camera's sensor size is 17.3 x 13.0 mm and the pixel size is 0.0043 mm. These parameters are needed to calculate the image resolution on the ground or, i.e., the ground sample distance (GSD) as affected by the flight altitude.

Figure 3. The quadrocopter UAV and the visible-light (RGB) camera used to acquire the remote images of the olive plantation.

In each flight, the UAV route was designed to continuously take photos at 1 second interval, resulting to a forward lap of 90% at least. In addition, a side lap of 60% was programmed. The speed flight was 3 m/s and the altitude flight was 100 meters in the first and third dates, and 50 meters in the second date. Due to eventual strong windy conditions, the 100-m flight was aborted in the second date. According to the results reported by (Torres-Sánchez et al. 2015), this inconsistence can be disregarded because both flight altitudes produces similar results in the context of agricultural-tree plantations. To fully cover the experimental field, the camera collected 840 and 420 RGB images of 1.90 and 3.81 cm/pixel of ground sample distance (GSD) at 50-m and 100-m flight altitude, respectively. The flight operations fulfilled the list of requirements established by the Spanish National Agency of Aerial Security (AESA), including pilot license, safety regulations and limited flight distance (AESA 2014). The UAV flights were authorized by the person in charge of the olive farm, as well. A screen shot of a flight planning is shown in the Figure 4.

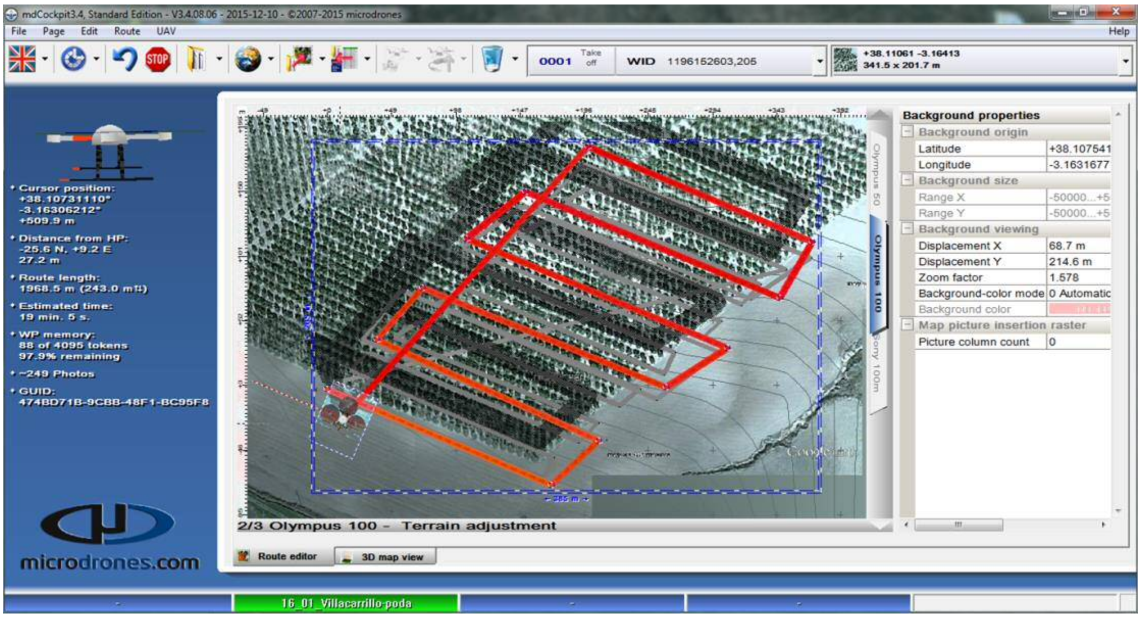

Figure 4. Screen shot of the Waypoint Editor module showing the flight planning.

2.3. Generation of the UAV image-based products: the 3D point cloud, the Digital Surface Model (DSM) and the image ortho-mosaic

By processing the set of UAV aerial images, three geo-spatial products of the studied olive plantation were produced: 1) the 3D point cloud file, by applying the structure-from-motion technique, 2) the Digital Surface Model (DSM), with height information, created from the 3D point cloud, and 3) the image ortho-mosaic, with RGB information of every pixel collected by the camera. In this research, the Agisoft PhotoScan Professional software, version 1.2.4 build 2399 (Agisoft LLC, St. Petersburg, Russia) was used for this task. The mosaicking process was fully automatic with the exception of the manual localization of six ground control points (GCP) used to georeferenced the products. The GCP were located in the corners and center of the field, and their coordinates were taken with a GPS device after the flight operations.

The automatic process involved three phases: 1) aligning images, 2) building field geometry, and 3) ortho-photo generation. The common points and the camera position for each image were located and matched, which facilitated the refinement of camera calibration parameters. Once the images were aligned, the cloud point was generated. Next, DSM was built based on the estimated camera position and the images themselves. This process requires a high computational resources and it can usually takes among 5 and 6 hours approximately due to use many high-resolutions photos. Finally, the images were projected over the DSM and the ortho-mosaic was generated (Figure 5). The DSM is a 3D polygon mesh that represents the overflown area and reflects the irregular geometry of the ground and the tree crowns. The DSM was joined to the ortho-mosaic as Tiff files, which produced 4-band multi-layer file (Red, Green, Blue and DSM). More information about the PhotoScan functioning is described in (Dandois and Ellis 2013).

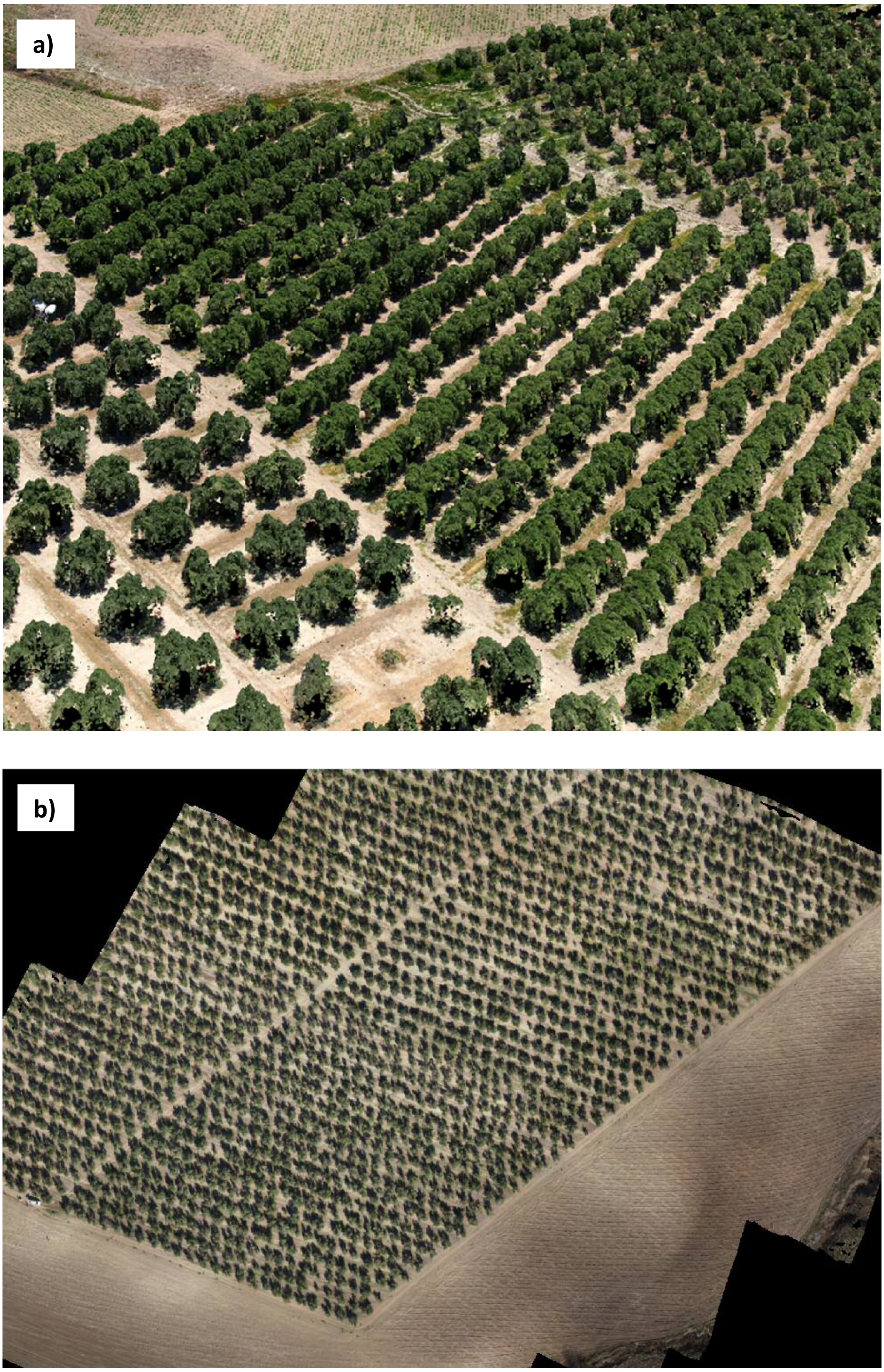

Figure 5. 3D cloud point image (a) and ortho-mosaicked image (b) produced from the UAV-based remotes images collected in the olive plantation.

2.4. Computing the olive tree geometric features by object-based image analysis (OBIA)

An innovative algorithm based on the OBIA paradigm was applied to the 4-band multi-layer file created in the previous phase in order to classify and identify each individual tree of the plantation and to compute their main geometric features, including the projected canopy area, the tree height (mean and maximum), and an estimation of the crown volume (Figure 6).

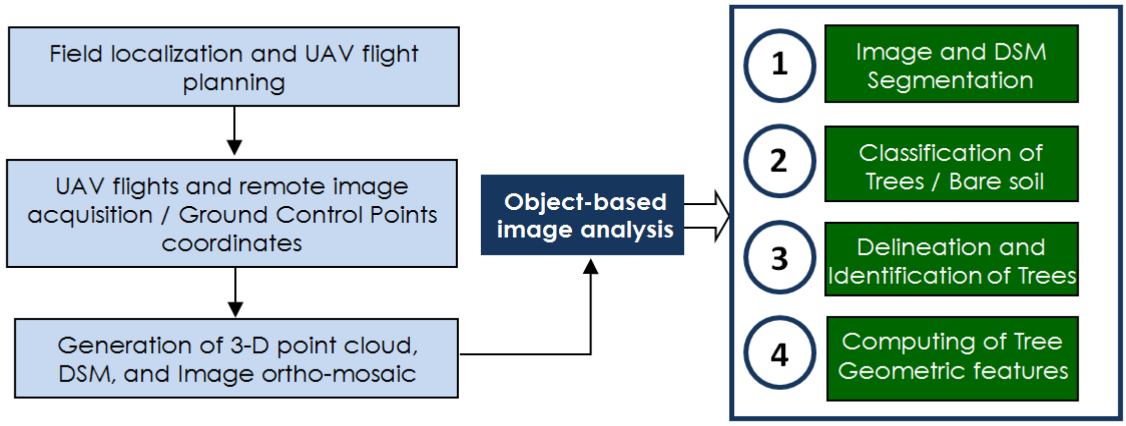

Figure 6. Outline of the UAV-based methodology to compute the olive tree geometric features.

The OBIA algorithm was created with the eCognition Developer 9 software (Trimble GeoSpatial, Munich, Germany) and it was adapted from the version described in (Torres-Sánchez et al. 2015), which reported overall accuracies over 90%. However, the procedure used here is original and includes improvements and variations related to the specifications of this research. After programing the algorithm, it is auto-adaptive to any plantation pattern and it runs fully automatic without the need of user intervention. The OBIA procedure was composed of a sequence of phases (Figure 7), described as follows:

Phase 1, Image and DSM segmentation: The 4-band (B, G, R, and DSM) multi-layer file was segmented into 1-m^2 square objects by using the chessboard segmentation process. In this version, only the DSM band was selected as reference for the segmentation, which weighted the variable “height” instead of the spectral information.

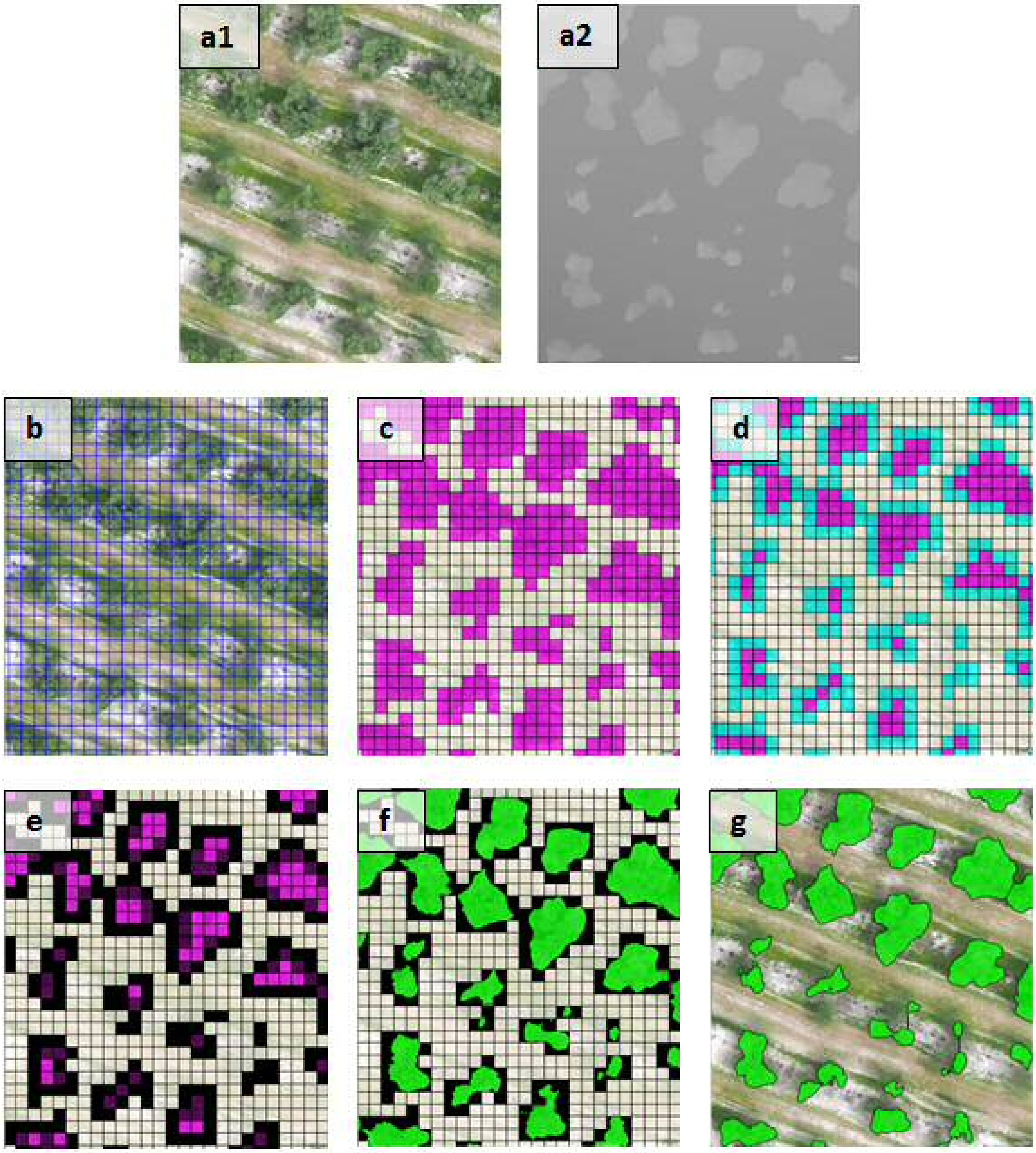

Figure 7. Partial views of the OBIA procedure: a) The 4-band multi-layer file with the RGB (a1) and the DSM (a2) layers; b) chessboard segmentation output; c) classification of the vegetation objects (pink color) and bare soil (white color) based on the difference of DSM (height) values; d), e) Refined of the borders of the vegetation objects through new pixel-based segmentations; f) Tree delineation; g) the tree and the bare-soil objects are separately joined, and the olive tree geometric features are computed and exported for further analysis.

Phase 2, Classification of trees and bare soil: The segmented objects with high values of DSM (height) standard deviation (SD > 0.1 m) were classified as trees and the remaining objects as bare soil.

Phase 3, Delineation and identification of trees: All the objects which had been classified as trees were analyzed at the pixel level. Then, the DSM value of each pixel was compared to the surrounding bare soil DSM values and classifying every pixel as tree or bare soil. Next, all the pixels classified as tree were joined into single objects and identified as individual trees.

Phase 4, Computing the tree geometric features: The geometric features (area, height and volume of the olive trees) were automatically calculated by applying a looping process in which each tree was individually identified and analyzed. The height of each tree pixel was obtained by comparing its DSM value to the DSM values of the surrounding bare soil pixels. Next, knowing the height of all the pixels of each tree, the tree mean and maximum heights were obtained for all the trees in the plot. Simultaneously, the tree volume was computed by adding up the volumes (multiplying pixel areas and heights) of all the pixels of each tree crown. Finally, the OBIA algorithm automatically exported the tree geometric features as vector (e.g., shapefile format) and table (e.g., excel or ASCII format) files for further analysis (Figure 8).

	Tree ID	Row	Column	X	Y	Pruning	Area (Date 1)	Area (Date 2)	Area (Date 3)	Height_max (Date 1)	Height_max (Date 2)	Height_max (Date 3)	Height_mean (Date 1)	Height_mean (Date 2)	Height_mean (Date 3)	Volume (Date 1)	Volume (Date 2)	Volume (Date 3)
1	1	1	1	485726	4217762	Traditional	15,38	12,44	17,24	3,81	3,72	3,55	2,87	2,79	2,50	44,09	34,74	43,16
2	2	1	2	485732	4217760	Traditional	15,88	9,61	16,69	4,10	4,31	4,14	3,01	2,86	2,68	47,75	27,52	44,68
3	3	1	3	485738	4217757	Traditional	13,98	10,77	14,58	3,91	3,62	3,60	2,53	2,48	2,38	35,42	26,68	34,68
4	...	...	...	...	...	...	...	...	...	...	...	...	...	...	...	...	...	...
5	217	10	1	485786	4217808	Adapted	15,34	5,16	11,13	4,37	4,04	4,43	2,86	2,57	2,82	43,81	13,28	31,43
6	218	10	2	485789	4217806	Adapted	14,96	5,46	12,26	3,81	3,84	3,97	2,93	2,77	2,89	43,81	15,15	35,45
7	219	10	3	485795	4217803	Adapted	12,64	7,62	13,02	4,53	3,77	3,45	2,51	2,49	2,11	31,73	18,99	27,43
8	...	...	...	...	...	...	...	...	...	...	...	...	...	...	...	...	...	...
9	433	19	1	485840	4217852	Mechanized	7,00	5,75	7,20	3,85	3,48	3,83	2,69	2,02	2,45	18,78	15,67	17,68
10	434	19	2	485846	4217851	Mechanized	10,11	10,20	13,64	4,31	3,58	3,79	2,70	2,62	2,84	27,28	26,73	31,97
11	435	19	3	485850	4217848	Mechanized	13,55	13,56	14,93	4,17	3,54	3,61	3,24	2,90	2,94	43,87	39,38	42,49
12	...	...	...	...	...	...	...	...	...	...	...	...	...	...	...	...	...	...
13	648	27	24	486017	4217841	Mechanized	6,06	5,93	6,30	3,48	3,34	3,54	2,52	2,45	2,14	15,27	14,52	15,46

Figure 8. A sample of the output data file computed at the tree level.

2.5. Data analysis and validation

The outputs delivered by the OBIA algorithm in the three studied dates were exported to the software JMP version 10 (SAS Institute Inc., Cary, NC, USA) in order to submit the data to statistical analysis. The variations of the tree projected canopy area, the tree mean and maximum height, and the tree crown volume as affected by the pruning treatment and the flight date were evaluated by performing a Tukey honest significant difference (Tukey-HSD) test at a significance level of 5% ($p \leq 0.05$) through a one-way analysis of variance (ANOVA).

In addition, quality of the DSM layers created in the three dates, which produces the 3D models of the olive trees, was evaluated by visually comparing the tree perimeter defined by the OBIA algorithm (based in the DSM layer) and the real tree perimeter observed in the RGB mosaicked image. As a result, global accuracy of the full procedure in each date was reported and the trees with uncorrected 3D reconstruction were removed from the subsequent statistical analysis in order to avoid imprecise conclusions.

3. Results

3.1. Evaluation of the procedure

The number and percentage of trees correctly computed in every studied date are shown in Table 1. This table summarizes that date 1 presented the highest accuracy values achieved in the characterization of the tree olives, being correctly computed the 92.6 % of the trees in the sub-plots corresponding to the traditional and adapted pruning treatments. Furthermore, the mechanized treatment presented an 85.7 % of accuracy. For the date 2, one month after pruning, the adapted treatment sub-plot showed a 75.5 % of well delineated trees and the mechanized reached until a 96.3 % of accuracy. Third, between 81.9 and 88.4 % of well delineated tree was achieved in the third date, having the mechanized treatment the highest value of all the treatments. Finally, the last column exposes the number and percentage of trees correctly delineated in the three dates (1-2-3), appearing values between 74.5 % for the adapted and 81.9 % for the mechanized pruning treatment.

Table 1. Number and percentage of olive trees correctly computed in every date.

Pruning Treatment	Number of trees	Date 1	Date 2	Date 3	Dates 1-2-3
Traditional	216	200 (92.6 %)	180 (83.3 %)	190 (88.0 %)	174 (80.6 %)
Adapted	216	200 (92.6 %)	163 (75.5 %)	177 (81.9 %)	161 (74.5 %)
Mechanized	216	185 (85.7 %)	208 (96.3 %)	191 (88.4 %)	177 (81.9 %)

Flight dates: Date 1 (Before pruning); Date 2 (After pruning), Date 3 (One year after pruning).

3.2. Influence of the pruning treatment in the tree geometry

The OBIA procedure reported the area, maximum height and volume of every olive tree in the three studied dates (Figures 9, 10 and 11, respectively), which can be plotted for descriptive analysis.

In the Figure 9 can be appreciated the obtained projected area values in every flight date. In the date 1, the lowest values for crown area projected are clearly founded in the mechanized treatment sub-plot. Next, after pruning, big differences appeared in the traditional and adapted pruning treatments sub-plots. However, there were not important changes for the trees that had been pruned in the mechanized way. Finally, the third date showed a notable growth for all the trees of the plot and besides the trees of the traditional and adapted pruning, that lost a large amount of foliage in relation to mechanized treatment, generally reached the values of the initial situation or date 1.

With respect to the changes produced on the maximum height values that are shown in the Figure 10, important differences appeared in relation to the mechanized pruning block between the first and second date. In this point, due to it was applied to a same pruning height class (3.5 to 4 meters in height), the date 2 exhibits a more homogeneity color distribution. Furthermore, the olive trees under this treatment didn´t experience a significant growth in height between the second and third date.

Thirdly, in relation to the values of volume in every date that are displayed in the Figure 11, as was expected, the pruning specially affected to the volumes values of the trees under traditional and adapted pruning treatments. Anyway, these trees that were pruned in a most aggressive way experienced the greatest growths between the second and third date.

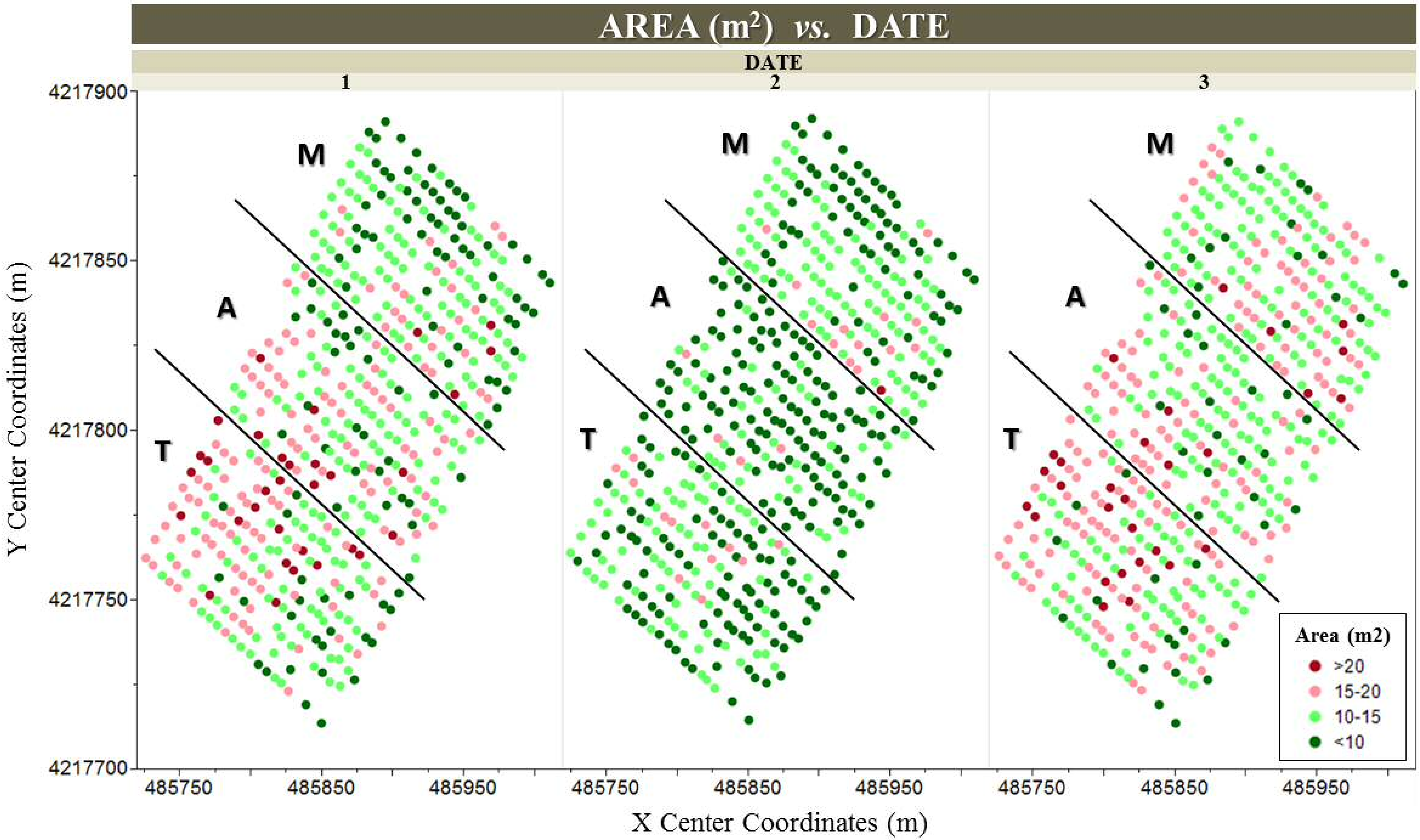

Figure 9. Olive tree projected area in the three studied dates: Date 1 (Before pruning), Date 2 (After pruning), and Date 3 (one year later after pruning). T: Traditional pruning; A: Adapted pruning; M: Mechanized pruning.

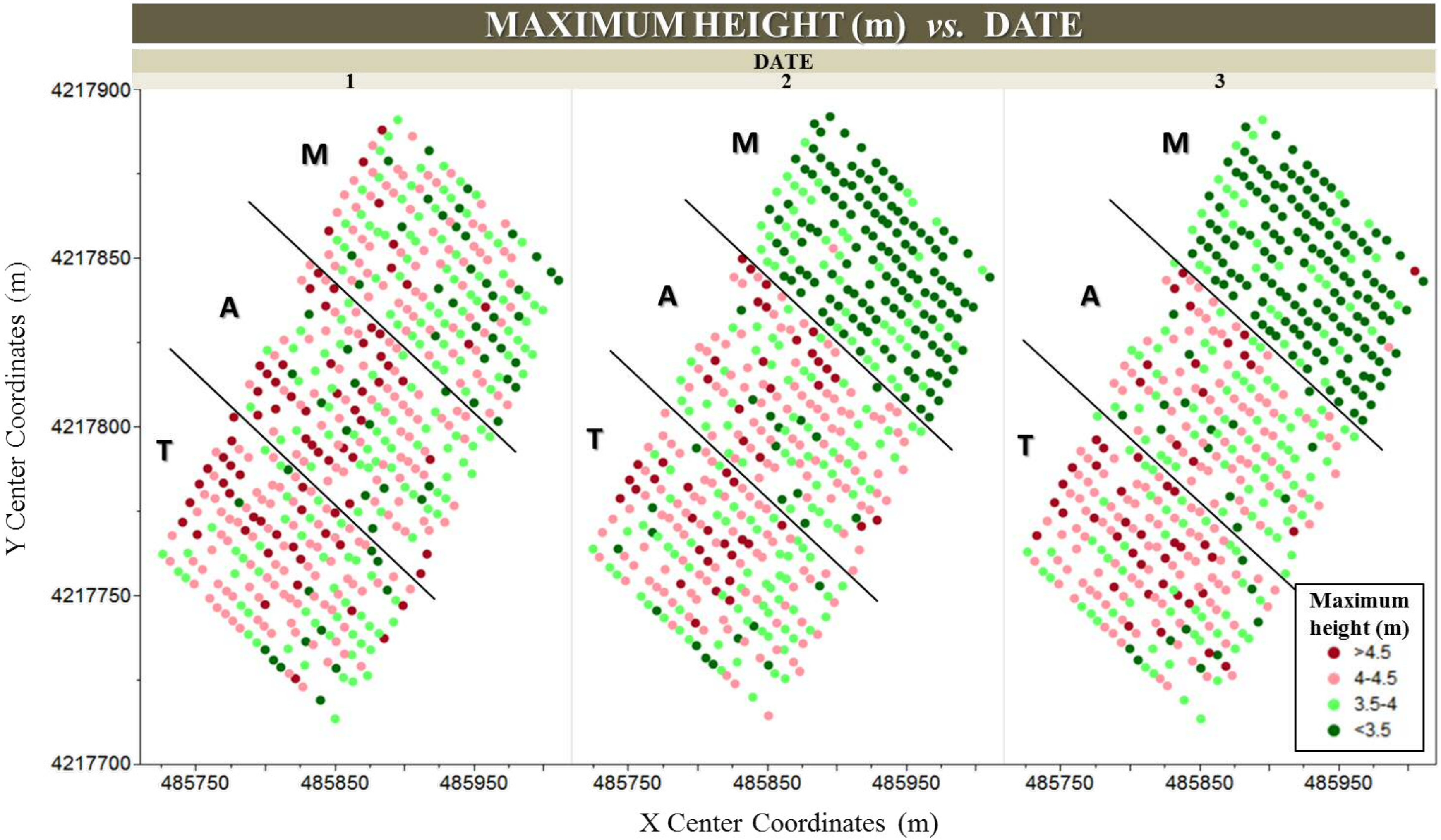

Figure 10. Olive tree maximum height in the three studied dates: Date 1 (Before pruning), Date 2 (After pruning), and Date 3 (one year later after pruning). T: Traditional pruning; A: Adapted pruning; M: Mechanized pruning.

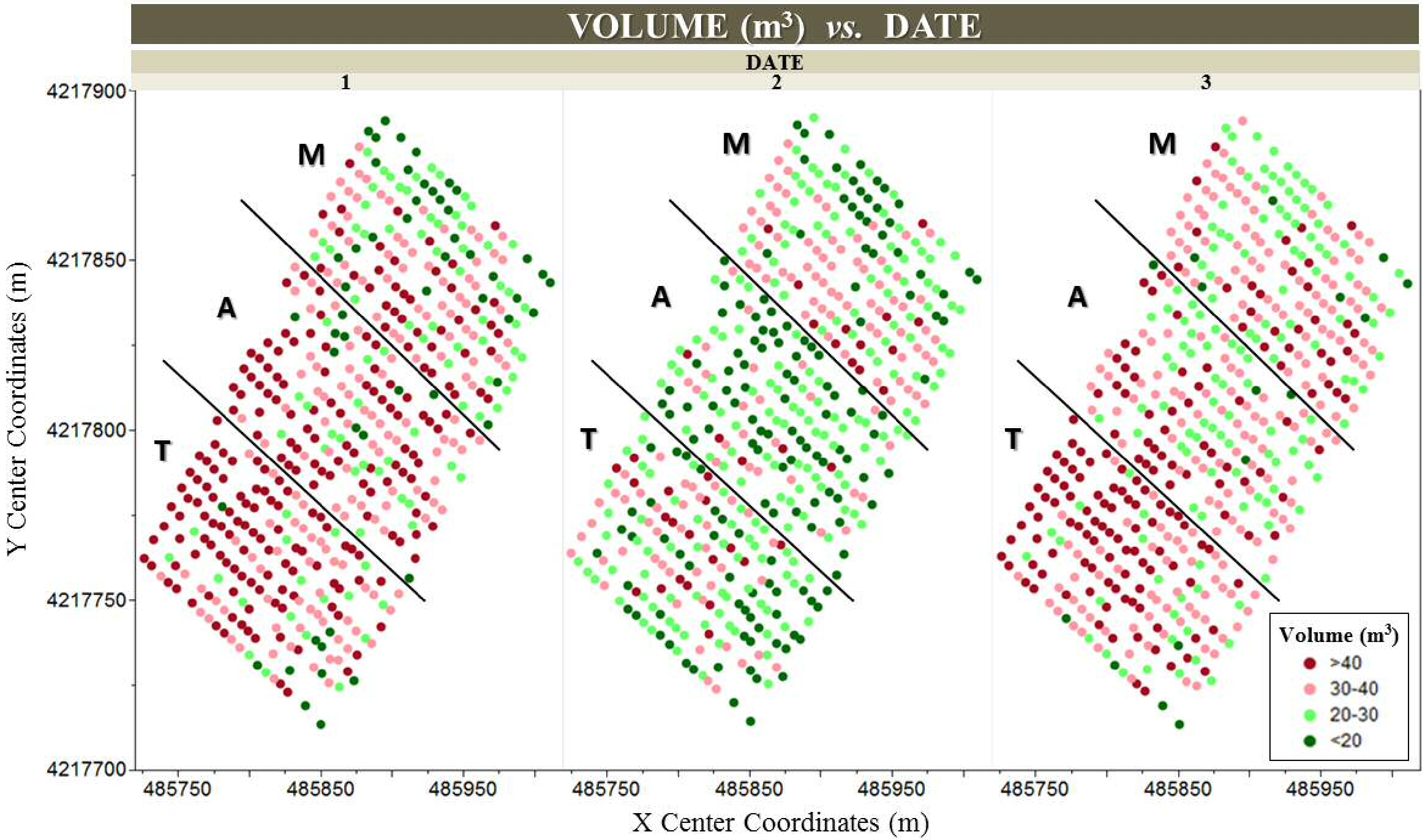

Figure 11. Olive tree volume in the three studied dates: Date 1 (Before pruning), Date 2 (After pruning), and Date 3 (one year later after pruning). T: Traditional pruning; A: Adapted pruning; M: Mechanized pruning.

Table 2 summarizes the mean values followed by their standard deviations of the projected canopy area, the maximum and mean heights, and the crown volume of the trees for each flight date and each pruning treatment. In the first flight date, significant differences appeared between the traditional and adapted pruning on the one hand, and mechanized pruning, on the other hand, being the mean values for the trees corresponding a this treatment lower than the other ones for all the analyzed variables.

The second date, regarding to the area, showed significant differences between the three pruning treatments. Then, mechanized treatment presented the highest mean value of area projected after pruning. However, in the second date the lowest height mean values corresponded to this treatment, appearing significant differences with respect to the other ones. Besides, the standard deviations corresponding to the maximum and mean height values presented higher differences among the three pruning treatments than in first date due to the homogeneity derived by a fixed cut height, being the standard deviation for the mechanized treatment half of the standard deviation for the other treatments. For the volume variable, the adapted pruning treatment proved to be significantly different from the other two treatments with a value of 22.72 m^3 (almost half of the shown value in the first analyzed date).

Finally, in the third date there were significant differences among the traditional pruning and the other ones for the area and volume variables. Furthermore, tree maximum and mean height presented differences among all the treatments. It is noticeable that the olive trees under traditional and adapted pruning treatments lost a highest amount of foliage with respect to the mechanized pruning and that, those trees experienced a major growth for all its variables, especially for area and volume.

Table 2. Mean and standard deviation for Area, Tree maximum height, Tree mean height and Volume tree as affected by pruning treatment and flight date.

Pruning Treatments	Date 1				Date 2				Date 3			
	Area (m^2)	Max Height (m)	Mean Height (m)	Volume (m^3)	Area (m^2)	Max Height (m)	Mean Height (m)	Volume (m^3)	Area (m^2)	Max Height (m)	Mean Height (m)	Volume (m^3)
Traditional	14.72 a ± 4.39	4.13 a ± 0.42	2.89 a ± 0.34	42.69 a ± 13.88	9.73 b ± 3.39	4.10 a ± 0.39	2.76 a ± 0.27	27.11 a ± 10.67	15.12 a ± 3.76	4.16 a ± 0.38	2.70 a ± 0.29	41.02 a ± 11.45
Adapted	13.94 a ± 4.00	4.13 a ± 0.45	2.87 a ± 0.34	40.18 a ± 12.88	8.38 c ± 2.78	4.08 a ± 0.37	2.70 a ± 0.24	22.72 b ± 8.10	13.71 b ± 3.25	4.03 b ± 0.39	2.50 b ± 0.30	34.30 b ± 9.03
Mechanized	11.61 b ± 3.61	3.90 b ± 0.41	2.72 b ± 0.34	31.91 b ± 11.53	10.72 a ± 3.34	3.40 b ± 0.20	2.61 b ± 0.15	28.12 a ± 9.35	13.97 b ± 2.95	3.32 c ± 0.24	2.34 c ± 0.22	32.78 b ± 7.65

Flight dates: Date 1 (Before pruning); Date 2 (After pruning), Date 3 (One year after pruning).

Different letters in a same column represent significant differences for the mean values at p-value < 0.05.

3.3. Multi-temporal variation of the tree geometry as affected by the pruning treatment

Table 3 presents the effect of the different pruning treatments (differences of dates 2 and 1), as well of the tree growth (differences of dates 3 and 2), regarding tree projected area (a), mean and maximum height (b) and crown volume (c). Besides, differences of date 3 and 1 also are quantified to compare the tree vegetative response along this research.

Analyzing the effects produced by the different pruning treatments on the olive trees (Date 2 – Date 1), important significant differences appeared among the trees under traditional and adapted pruning on the one hand, and the mechanized pruning on the other hand, for all variables except for tree mean heights. In this point, the adapted pruning treatment resulted to be the most aggressive, presenting the greatest loss of crown volume (-17.46 m^3). The standard deviations showed a higher variability for the traditional and adapted treatments between these dates due to the pruning typologies.

In relation to the olive tree growth response since these were pruned until one year later (Date 3 – Date 2) it can be appreciated important differences among the three treatments. Moreover, it is important to point out that the trees that were pruned in a mechanized form experienced a minor growth than the other ones. Nevertheless, in general, there were not high growths in height in this point.

Finally, to compare the mean values presented in the last flight date with the initial situation (Date 3 – Date 1), significant differences were posed among the three treatments and analyze variables. The trees corresponding to the mechanized pruning treatment experienced an increase of 0.87 m^3 in volume with respect to the initial situation. On the other hand, and because of adapted pruning typology, the olive trees under this treatment presented the greatest differences in relation to the volume variable and not reached the initial situation mean values (-5.88 m^3).

Table 3. Mean and standard deviation of multi-temporal differences for Area, Tree maximum height, Tree mean height and Volume tree as affected by pruning treatment.

Pruning Treatment	Date 2 – Date 1				Date 3 – Date 2				Date 3 – Date 1			
	Area (m^2)	Max Height (m)	Mean Height (m)	Volume (m^3)	Area (m^2)	Max Height (m)	Mean Height (m)	Volume (m^3)	Area (m^2)	Max Height (m)	Mean Height (m)	Volume (m^3)
Traditional	-5.00 a ± 2.87	-0.03 b ± 0.31	-0.13 a ± 0.25	-15.58 a ± 8.19	5.39 a ± 2.03	0.06 a ± 0.20	-0.05 a ± 0.17	13.90 a ± 6.06	0.39 b ± 2.32	0.03 a ± 0.28	-0.18 a ± 0.25	-1.68 b ± 6.80
Adapted	-5.56 a ± 2.68	-0.05 b ± 0.38	-0.17 a ± 0.31	-17.46 a ± 8.73	5.34 a ± 1.71	-0.05 b ± 0.24	-0.20 b ± 0.22	11.58 b ± 4.98	-0.23 c ± 2.50	-0.10 b ± 0.36	-0.37 b ± 0.31	-5.88 c ± 7.81
Mechanized	-0.89 b ± 1.40	-0.51 a ± 0.40	-0.11 a ± 0.25	-3.79 b ± 4.93	3.25 b ± 1.50	-0.08 b ± 0.19	-0.26 c ± 0.17	4.66 c ± 4.60	2.35 a ± 1.76	-0.59 c ± 0.42	-0.37 b ± 0.29	0.87 a ± 6.47

Flight dates: Date 1 (Before pruning); Date 2 (After pruning), Date 3 (One year after pruning).

Different letters in a same column represent significant differences for the mean values at p-value < 0.05.

The tree projected area, maximum height and volume differences due to the several pruning treatments were analyzed in a graphic way and for every olive tree by comparing the second and first date (2-1) on the one hand, and the third and second date (3-2), on the other hand (Figures 12, 13 and 14).

Figure 12 displays the area differences where can be seen how the sub-plot concerned to the mechanized pruning treatment experienced the lowest differences values after pruning. Furthermore, by comparing the area growths from date 2 until date 3, the trees of this treatment experienced a minor growth than the other ones. It can be also concluded that the trees were pruned in a most aggressive way experienced a greater growth.

In relation to the maximum tree height values, the Figure 13 exhibits important changes between the dates 2 and 1, especially for the mechanized pruning treatment. As this pruning treatment mainly removed the branches that were located at 3.5 to 4 meters in height; it produced the highest differences for this variable. However, this sub-plot presented differences from minimum to low between dates 2 to 3.

Figure 14 shows the volume differences among analyzed dates and pruning treatments and as it has been described above, the trees that lost more foliage experienced a highest crown volume growth.

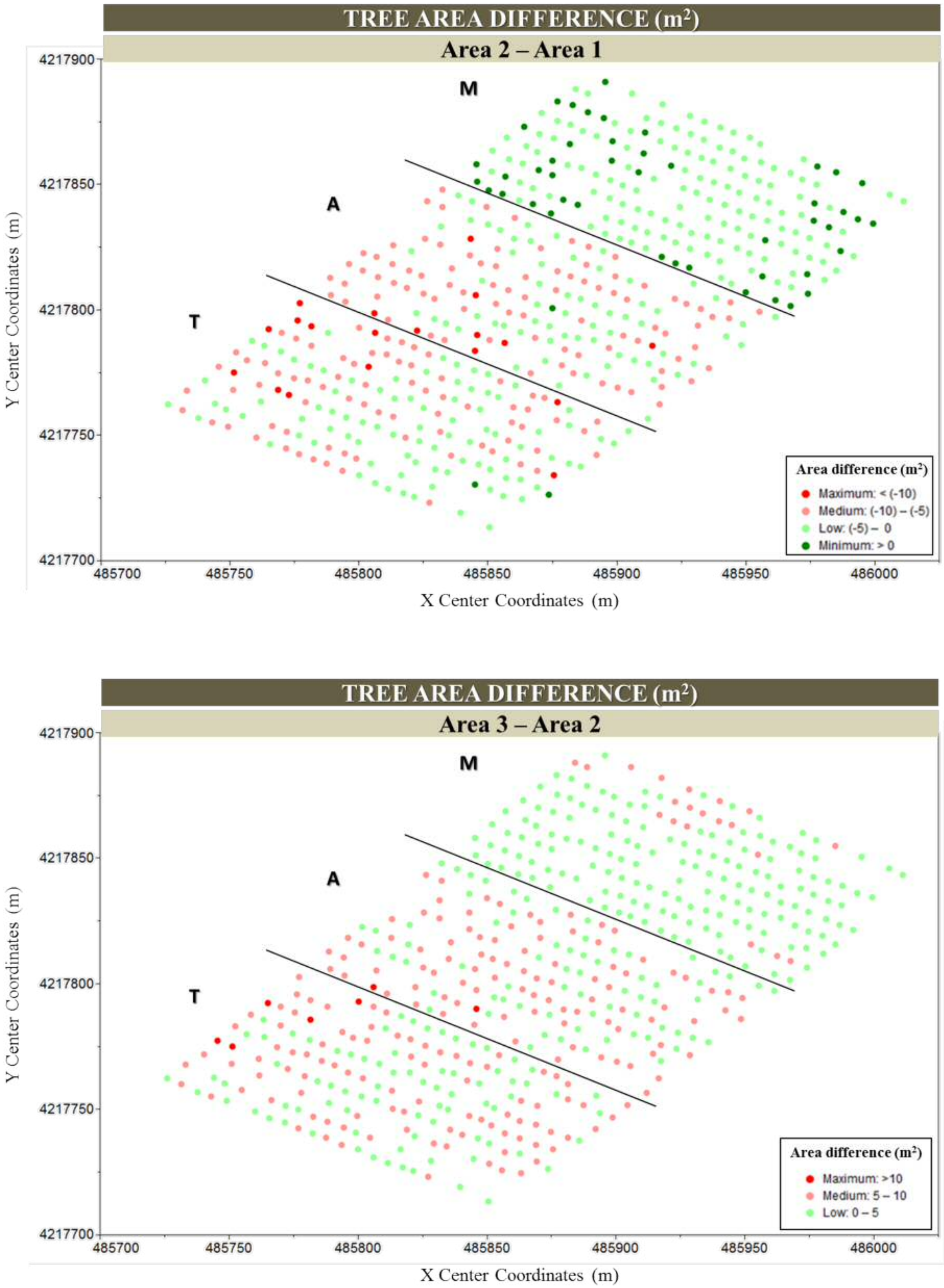

Figure 12. Assessment of pruning influence (differences of dates 2 and 1) and tree growth (differences of dates 3 and 2) regarding olive tree projected area (m^2). T: Traditional pruning; A: Adapted pruning; M: Mechanized pruning.

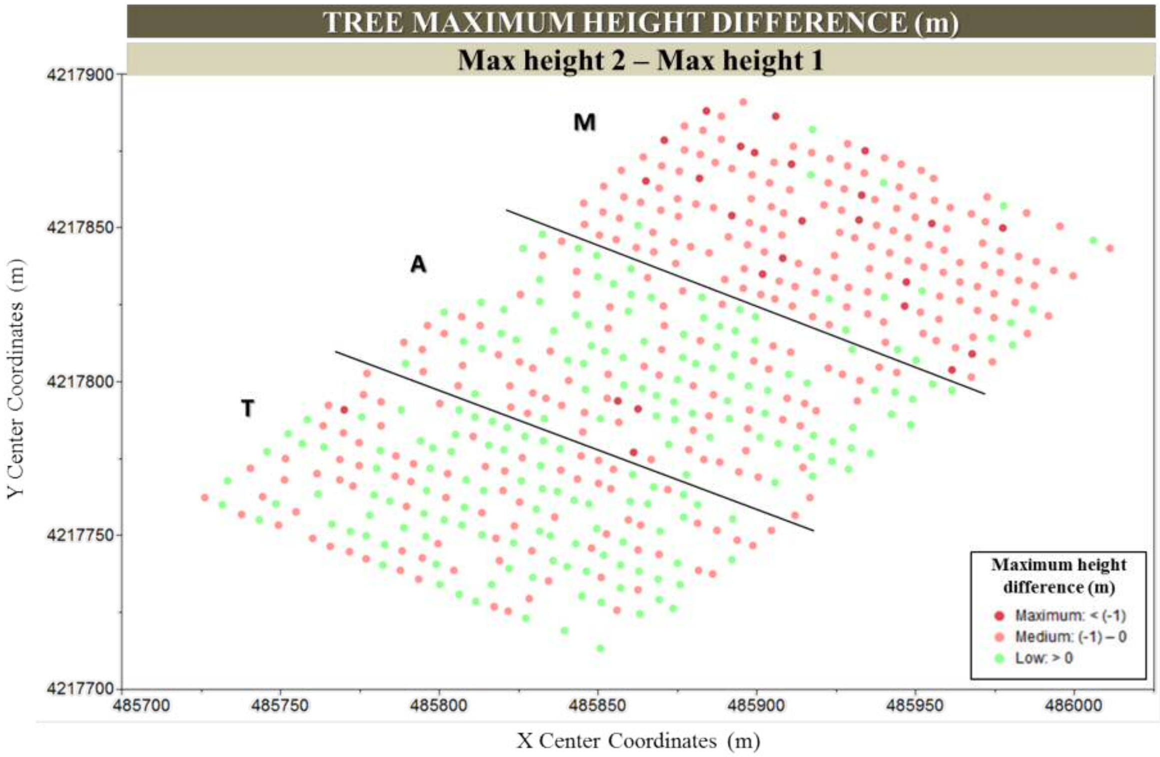

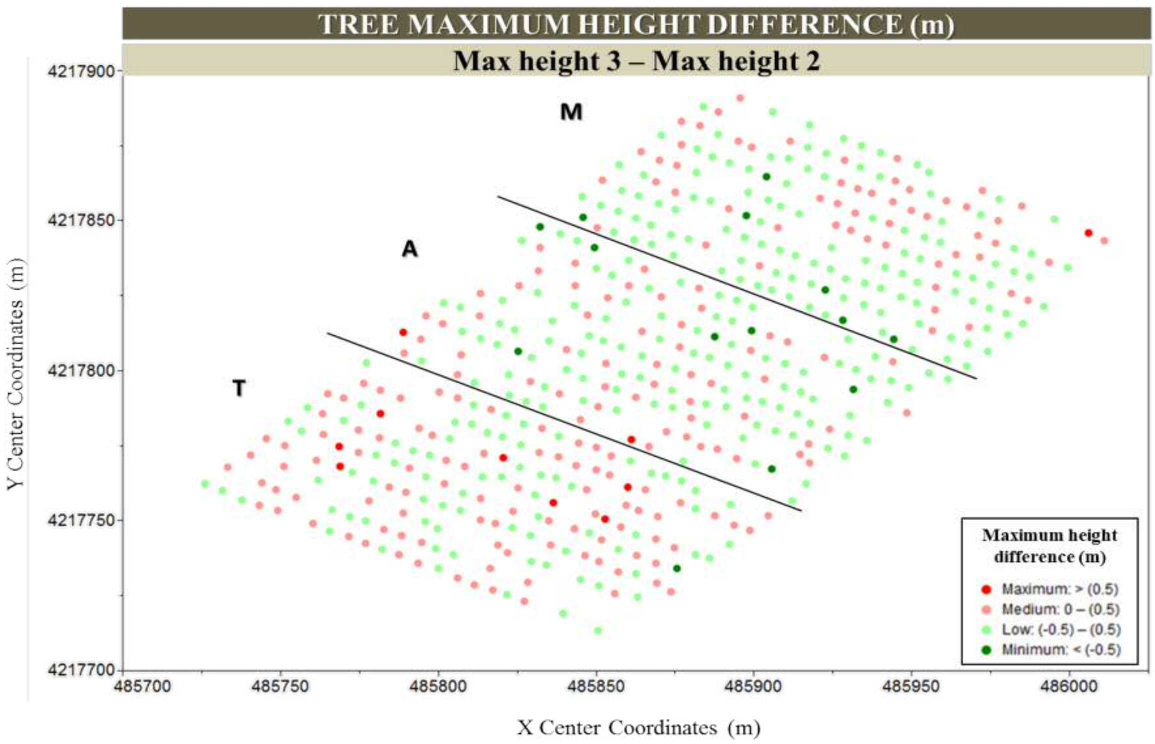

Figure 13. Assessment of pruning influence (differences of dates 2 and 1) and tree growth (differences of dates 3 and 2) regarding olive tree maximum height (m). T: Traditional pruning; A: Adapted pruning; M: Mechanized pruning.

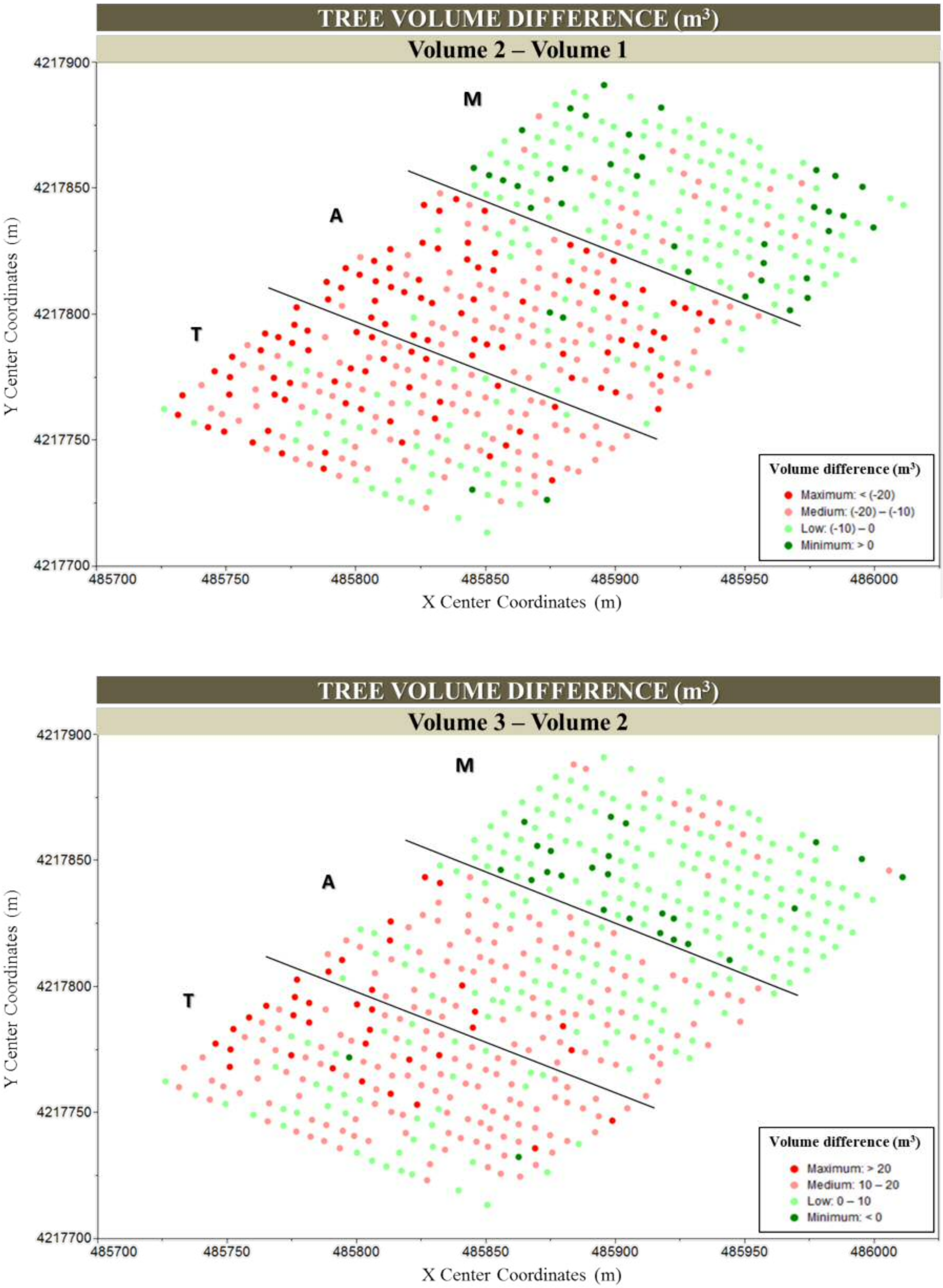

Figure 14. Assessment of pruning influence (differences of dates 2 and 1) and tree growth (differences of dates 3 and 2) regarding olive tree volume (m^3). T: Traditional pruning; A: Adapted pruning; M: Mechanized pruning.

4. Discussion

In relation to the accuracy of the procedure used in this investigation, it was checked that the olive trees that were not correctly delineated were located in the area where the DSM had poorer quality and it caused the algorithm to fail in the delineation of these trees. Furthermore, the olive trees under the adapted treatment presented the lowest percentages of tree correctly delineated from the date 2, because in this treatment the crown tree was strongly modified creating big gaps in the crown center. This fact complicated the tree delineate task to the algorithm. Anyway, the olive tree delineation accuracy could be improved by using spectral as well as DSM information (Torres-Sánchez et al. 2015).

It should be emphasized that in the initial situation, when any pruning treatment had been performed yet, it was observed that the trees corresponding to the mechanized pruning sub-plot were smaller (minor area, minor height and next, minor volume) than the trees of the other treatments. This might be because of they were located in the highest area of the plot where the soils could be less fertile. Although it would be necessary to perform a more detailed study of this issue to establish conclusions, the trees under traditional treatment which were located in the lowest plot area presented the highest values in this date.

After pruning, high differences appeared in the trees under traditional and adapted pruning treatments for the projected area variable. However, in this point there were not important changes for the trees that had been pruned in the mechanized way mainly due to the typology of this pruning (the crown was cut obliquely), whose effects can´t be detected when the crown area is projected. With respect to the tree height values important differences were detected for the trees under mechanized pruning between the first and second date, since in this pruning the branches located at a height from 3.5 to 4 meters were removed which produced a uniform pruning height in this sub-plot. Furthermore, and as was expected, the lowest volume values corresponded to the trees under traditional and adapted pruning treatments where a large amount of foliage was removed.

The vegetative growth was quantified almost a year after pruning being assessed the response of every tree after realizing the three pruning treatments. In this point was checked that the olives trees which were affected by a most aggressive pruning (adapted and traditional) experienced the highest volume growths. Nevertheless, the olive trees under mechanized treatment kept a more constant growth (Tombesi et al. 2002).

Thus, this research demonstrated that the combination of taking images by UAV technology together with object-based image analysis (OBIA) generated high-throughput monitoring in order to quantify the influence of three different pruning treatments on tree olive architecture. The results obtained underlined that this methodology allows carrying out numerous possibilities in relation to the orchard woody crops management.

Orchard architecture offers us information about tree biomass (Bendig et al. 2014; Velázquez-Martí et al. 2011), crown porosity (Castillo-Ruiz et al. 2016), and interception of solar irradiation needed to estimate productivity or irrigation requirement (Connor et al. 2014; Larbi et al. 2014; Mariscal et al. 2000), among other physiological aspects. For example, Cherbiy-Hoffmann et al. (2012) checked in a large olive hedgerow that oil production is limited by low solar radiation within the canopy. Castillo-Ruiz et al. (2016) presented an accurate and reliable method based on transmitted radiation measurements in order to assess the porosity of traditional olive trees under different pruning treatments. On the other side, Gómez et al. (2002) followed two objectives related with the porosity of the tree crown: characterize the rainfall distribution beneath olive canopies and determining the zones of rainfall concentration and estimating the magnitude of the water fluxes in these zones.

In addition, quantifying the effect of pruning on the tree volume can give us a value of the amount of pruning residues. In relation to the management of this task, increasingly the application of these rests on the field in no-till systems and mainly in steep areas, a common practice in precision agriculture, in order to reduce the soil erosion and improving the organic matter content. There are several works that studied the effects of these techniques on the olive grove soils (Calatrava and Franco 2011; Rodríguez-Lizana et al. 2008; Gómez-Muñoz et al. 2016; Repullo et al. 2012).

Concluding this paragraph, thanks to the presented methodology in this master´s thesis we can quantify the volume of pruning residues in a plot in order to take decisions about the agricultural and ecological effects that would have to leave these rests in the plot soil.

Alternatively, olive tree 3D models can also provide useful information about potential crop yield. It would be interesting to try developing prediction models to connect the volume of the tree crown and the density of its canopy with its yield, although it is a complex issue since it depends on a large number of factors. Investigations have addressed the relations between pruning treatments and tree production. Tombesi et al. (2002) studied the influence of canopy density after applying several pruning intensities on efficiency of trunk shaker on olive mechanical harvesting where a moderate and heavy annual pruning helped mechanical fruit harvesting because of a larger fruit size, a less dense canopy and a regular distribution without bundling and overlapping of fruity shoots. Nevertheless, lack of pruning caused the crown to grow upward and away from the main branches which resulted in defoliation due to lack of light and parasitic attack. Therefore, Farinelli et al. (2011) assessed the effect of a mechanical pruning of adult olive trees and its influence on yield and on efficiency of mechanical harvesting. Thus, knowing the produced effects by different pruning treatments on architecture tree can provides us useful information about the yield of an orchard olive.

Finally, other interesting application of knowing the geometrical features of the olive crown tree can be the establishment of adjusted doses of plan protection products. In the last years and due to the publication in 2009 of the European Directive for a Sustainable Use of Pesticides, 2009/128/CE of the European Parliament and the Council, EU members have tried to reduce the associated risks during the pesticide applications. Most efforts have focused in woody crops such as orchards, olive tree and vineyards plantations where procedures to identify the suitable doses and volume rates have been established to avoid the spray drift and runoff. It is known that pesticide spray application is an important preventive task that contributes to avoid the yield losses because of organisms and pests that harm the crops. If this application is not adjusted to the crop architecture, problems for the environment due to pollution, traces of pesticides in food and health issues in human operators could be generated. In this way, several researches have addressed questions to search how to apply the most adjusted dose application. Miranda-Fuentes et al. (2016) assessed the optimal liquid volume to be sprayed on isolated olive trees according to their canopy volumes. In a previous research (Miranda-Fuentes et al. 2015), three simple methods were evaluated to determine their accuracy in order to characterize the tree crown as alternative to LiDAR technology. Furthermore, Planas et al. (2015) presented *Dosafrut*, a new concept to determine the application volume rate of pesticide treatments in fruit orchards. Other authors as (Siegfried et al. 2007) carried out a research in precision viticulture about the dosage of plant protection products adapted to leaf area index (LAI) in contrast to standard dosage. Also in viticulture, Gil et al. (2007) and Llorens et al. (2010) proposed the use of ultrasonic sensors and proportional electro-valves to achieve a significant reduction in spray volume while maintaining coverage and penetration rates similar to conventional methods.

5. Conclusions

This investigation has demonstrated the possibilities of the UAV technology to carry out high-throughput monitoring through multitemporal analysis on architecture olive orchard affected by different pruning treatments, offering a very valuable alternative to hard and inefficient field work.

The combination of taking images in three flight dates (before pruning, one month after pruning and almost a year after pruning) by a UAV, and using object-based image analysis (OBIA), allowed to quantify the differences produced by three different pruning treatments (traditional, adapted and mechanized) on the studied crown geometrical features of every tree in the plot: crown projected area, tree height and crown volume. On the other hand, it also could be assessed the tree growth response after pruning along the research studying the differences among the trees of every treatment.

The OBIA algorithm used achieved high percentages of trees correctly defined in all analyzed dates except in the areas where DSM had been generated with a lower accuracy. It was checked the olive trees located under adapted pruning, the treatment where a large amount of foliage was removed, showed the highest foliage loss after pruning followed by trees under traditional pruning, but also experienced higher growths than the other ones, being quantified this response vegetative almost a year after pruning. Due to the pruning mechanized typology, the trees under this treatment kept a more constant vegetative growth along the research.

Due to the possibilities that are presented in this masther´s thesis, this research opens the doors towards a wide study area in the agronomical sector, being presented a interesting methodology with promising applications in precision oliviculture although also possibly in other woody crops.

6. Acknowledgments

This research was partially financed by the CSIC-Intramural-Project (ref. 201640E034). Title: "Architecture and monitoring of woody crops using imagery from unmanned aerial vehicles for a sustainable application of pesticides". The author thanks Dr. Francisca López-Granados, Jorge Torres-Sánchez, Dr. Ana Isabel de Castro-Megías and Irene Borra-Serrano (imaPing group: www.ias.csic.es/imaping) for their very helpful assistance during the field works and their contributions in this research.

7. References

AESA. (2014). Aerial work - Legal Framework. http://www.seguridadaerea.gob.es/LANG_EN/cias_empresas/trabajos/rpas/marco/default.aspx. Accessed 30 September 2016.

Bendig, J., Bolten, A., Bennertz, S., Broscheit, J., Eichfuss, S. & Bareth, G. (2014). Estimating Biomass of Barley Using Crop Surface Models (CSMs) Derived from UAV-Based RGB Imaging. *Remote Sensing*, *6*, 10395–10412. doi:10.3390/rs61110395 (open access).

Blaschke, T., Hay, G. J., Kelly, M., Lang, S., Hofmann, P., Addink, E., Feitosa, R. Q., Meer, F., Werff, H., Coillie, F. & Tiede, D. (2014). Geographic Object-Based Image Analysis – Towards a new paradigm. *ISPRS Journal of Photogrammetry and Remote Sensing*, *87*, 180–191.

Calatrava, J. & Franco, J. A. (2011). Using pruning residues as mulch: Analysis of its adoption and process of diffusion in Southern Spain olive orchards. *Journal of Environmental Management*, *92*, 620–629.

Castillo-Ruiz, F., Castro-Garcia, S., Blanco-Roldan, G., Sola-Guirado, R. & Gil-Ribes, J. (2016). Olive Crown Porosity Measurement Based on Radiation Transmittance:

An Assessment of Pruning Effect. *Sensors*, *16*, 723. doi:10.3390/s16050723 (open access).

Castillo-Ruiz, F. J., Castro-Garcia, S., Blanco-Roldan, G. L., Sola-Guirado, R. R. & Gil-Ribes, J. A. (2016). Olive Crown Porosity Measurement Based on Radiation Transmittance: An Assessment of Pruning Effect. *Sensors*, *16*, 723. doi:10.3390/s16050723 (open access).

Cherbiy-Hoffmann, S. U., Searles, P. S., Hall, A. J. & Rousseaux, M. C. (2012). Influence of light environment on yield determinants and components in large olive hedgerows following mechanical pruning in the subtropics of the Southern Hemisphere. *Scientia Horticulturae*, *137*, 36–42.

Connor, D. J., Gómez-del-Campo, M., Rousseaux, M. C. & Searles, P. S. (2014). Structure, management and productivity of hedgerow olive orchards: A review. *Scientia Horticulturae*, *169*, 71–93.

Dandois, J. P. & Ellis, E. C. (2013). High spatial resolution three-dimensional mapping of vegetation spectral dynamics using computer vision. *Remote Sensing of Environment*, *136*, 259–276.

Díaz-Varela, R. A., de la Rosa, R., León, L. & Zarco-Tejada, P. J. (2015). High-Resolution Airborne UAV Imagery to Assess Olive Tree Crown Parameters Using 3D Photo Reconstruction: Application in Breeding Trials. *Remote Sensing*, *7*, 4213–4232. doi:10.3390/rs70404213 (open access).

Díaz-Varela, R. A., Zarco-Tejada, P. J., Angileri, V. & Loudjani, P. (2014). Automatic identification of agricultural terraces through object-oriented analysis of very high resolution DSMs and multispectral imagery obtained from an unmanned aerial vehicle. *Journal of Environmental Management*, *134*, 117–126.

Farinelli, D., Onorati, L., Ruffolo, M. & Tombesi, A. (2011). Mechanical pruning of adult olive trees and influence on yield and on efficiency of mechanical harvesting. *Acta Horticulturae*, *924*, 203–209.

Ferguson, L., Glozer, K., Crisosto, C., Rosa, U. A., Castro-Garcia, S., Fichtner, E. J., Guinard, J. X., Lee, S. M., Krueger, W. H., Miles, J. A & Burns, J. K. (2012). Improving canopy contact olive harvester efficiency with mechanical pruning. *Acta Horticulturae*, *965*, 83–87.

Fernández-Sarría, A., Martínez, L., Velázquez-Martí, B., Sajdak, M., Estornell, J. & Recio, J. A. (2013). Different methodologies for calculating crown volumes of Platanus hispanica trees using terrestrial laser scanner and a comparison with classical dendrometric measurements. *Computers and Electronics in Agriculture*, *90*, 176–185.

Gil, E., Escolà, A., Rosell, J. R., Planas, S. & Val, L. (2007). Variable rate application of plant protection products in vineyard using ultrasonic sensors. *Crop Protection*, *26*, 1287–1297.

Gómez, J. A., Vanderlinden, K., Giráldez, J. V. & Fereres, E. (2002). Rainfall concentration under olive trees. *Agricultural Water Management*, *55*, 53–70.

Gómez-Muñoz, B., Valero-Valenzuela, J. D., Hinojosa, M. B. & Garcia-Ruiz, R. (2016). Management of tree pruning residues to improve soil organic carbon in olive groves. *European Journal of Soil Biology*, *74*, 104–113.

Herwitz, S. R., Johnson, L. F., Dunagan, S. E., Higgins, R. G., Sullivan, D. V., Zheng, J., Lobitz, B. M., Leung, J. G., Gallmeyer, B. A., Aoyagi, M., Slye, R. E. & Brass, J. A. (2004). Imaging from an unmanned aerial vehicle: agricultural surveillance and decision support. *Computers and Electronics in Agriculture*, *44*, 49–61.

Huete, M.D. & Marmolejo, J. A. (2016). Modelling the number of olive groves in Spanish municipalities. *Spanish Journal of Agricultural Research*, *14*, e0201.

Laliberte, A. S. & Rango, A. (2011). Image Processing and Classification Procedures for Analysis of Sub-decimeter Imagery Acquired with an Unmanned Aircraft over Arid Rangelands. *GIScience & Remote Sensing*, *48*, 4–23.

Larbi, A., Vázquez, S., El-Jendoubi, H., Msallem, M., Abadía, J., Abadía, A. & Morales, F. (2014). Canopy light heterogeneity drives leaf anatomical, eco-physiological, and photosynthetic changes in olive trees grown in a high-density plantation. *Photosynthesis Research*, *123*, 141–155.

Llorens, J., Gil, E., Llop, J. & Escolà, A. (2010). Variable rate dosing in precision viticulture: Use of electronic devices to improve application efficiency. *Crop Protection*, *29*, 239–248.

MAGRAMA. (2015). Statistical yearbook, Technical report. Ministry of agriculture, food and environment. http://www.magrama.gob.es/es/estadistica/temas/estadisticas-agrarias/. Accessed 14 August 2016.

Mariscal, M. J., Orgaz, F. & Villalobos, F. J. (2000). Modelling and measurement of radiation interception by olive canopies. *Agricultural and Forest Meteorology*, *100*, 183–197.

Mecaolivar. (2014). www.uco.es/cemtro/index.php/innovacion/item/45-proyecto-mecaolivar. Accessed 30 September 2016.

Miranda-Fuentes, A., Llorens, J., Gamarra-Diezma, J. L., Gil-Ribes, J. A. & Gil, E. (2015). Towards an Optimized Method of Olive Tree Crown Volume Measurement. *Sensors*, *15*, 3671–3687. doi:10.3390/s150203671 (open access).

Miranda-Fuentes, A., Llorens, J., Rodríguez-Lizana, A., Cuenca, A., Gil, E., Blanco-Roldán, G. L. & Gil-Ribes, J. A. (2016). Assessing the optimal liquid volume to be sprayed on isolated olive trees according to their canopy volumes. *Science of The Total Environment*, *568*, 296–305.

Peña, J. M., Torres-Sánchez, J., Castro, A. I. de, Kelly, M. & López-Granados, F. (2013). Weed Mapping in Early-Season Maize Fields Using Object-Based Analysis of Unmanned Aerial Vehicle (UAV) Images. *PLOS ONE*, *8*, e77151. doi:10.1371/journal.pone.0077151 (open access).

Planas, S., Sanz, R., Camp, F., Solanelles, F. & Rosell, J. R. (2015). The new concept of dose adjustment in tree crops. *Julius-Kühn-Archiv*, *448*, 64-65.

Qin, R. (2014). An Object-Based Hierarchical Method for Change Detection Using Unmanned Aerial Vehicle Images. *Remote Sensing*, *6*, 7911–7932. doi:10.3390/rs6097911 (open access).

Repullo, M. A., Carbonell, R., Hidalgo, J., Rodríguez-Lizana, A. & Ordóñez, R. (2012). Using olive pruning residues to cover soil and improve fertility. *Soil and Tillage Research*, *124*, 36–46.

Rodríguez-Lizana, A., Espejo-Pérez, A. J., González-Fernández, P. & Ordóñez-Fernández, R. (2008). Pruning Residues as an Alternative to Traditional Tillage to Reduce Erosion and Pollutant Dispersion in Olive Groves. *Water, Air, and Soil Pollution*, *193*, 165–173.

Rosell, J. R. & Sanz, R. (2012). A review of methods and applications of the geometric characterization of tree crops in agricultural activities. *Computers and Electronics in Agriculture*, *81*, 124–141.

Rovira-Más, F., Zhang, Q. & Reid, J. F. (2008). Stereo vision three-dimensional terrain maps for precision agriculture. *Computers and Electronics in Agriculture*, *60*, 133–143.

Siegfried, W., Viret, O., Huber, B. & Wohlhauser, R. (2007). Dosage of plant protection products adapted to leaf area index in viticulture. *Crop Protection*, *26*, 73–82.

Tombesi, A., Boco, M., Pilli, M. & Farinelli, D. (2002). Influence of canopy density on efficiency of trunk shaker on olive mechanical harvesting. *Acta Horticulturae*, *586*, 291–294.

Torres-Sánchez, J., López-Granados, F., Serrano, N., Arquero, O. & Peña, J. M. (2015). High-Throughput 3-D Monitoring of Agricultural-Tree Plantations with Unmanned Aerial Vehicle (UAV) Technology. *PLOS ONE*, *10*, e0130479. doi:10.1371/journal.pone.0130479 (open access).

Torres-Sánchez, J., Peña, J. M., de Castro, A. I. & López-Granados, F. (2014). Multi-temporal mapping of the vegetation fraction in early-season wheat fields using images from UAV. *Computers and Electronics in Agriculture*, *103*, 104–113.

Velázquez-Martí, B., Fernández-González, E., López-Cortés, I. & Salazar-Hernández, D. M. (2011). Quantification of the residual biomass obtained from pruning of trees in Mediterranean olive groves. *Biomass and Bioenergy*, *35*, 3208–3217.

Villalobos, F. J., Testi, L., Hidalgo, J., Pastor, M. & Orgaz, F. (2006). Modelling potential growth and yield of olive (*Olea europaea* L.) canopies. *European Journal of Agronomy*, *24*, 296–303.

West, P. W. (2009). Tree and Forest Measurement. Berlin, Heidelberg: Springer Berlin Heidelberg. http://link.springer.com/10.1007/978-3-540-95966-3. Accessed 20 April 2016.

Xiang, H. & Tian, L. (2011). Development of a low-cost agricultural remote sensing system based on an autonomous unmanned aerial vehicle (UAV). *Biosystems Engineering*, *108*, 174–190.

Xu, C., Lu, Z., Xu, G., Feng, Z., Tan, H. & Zhang, H. (2015). 3D Reconstruction of Tree-Crown Based on the UAV Aerial Images. *Mathematical Problems in Engineering*, *2015,* ID 318619. doi:10.1155/2015/318619 (open access).

Zarco-Tejada, P. J., Diaz-Varela, R., Angileri, V. & Loudjani, P. (2014). Tree height quantification using very high resolution imagery acquired from an unmanned aerial vehicle (UAV) and automatic 3D photo-reconstruction methods. *European Journal of Agronomy*, *55*, 89–99.

Zhang, C. & Kovacs, J. M. (2012). The application of small unmanned aerial systems for precision agriculture: a review. *Precision Agriculture*, *13*, 693–712.

Zheng, G. & Moskal, L. M. (2009). Retrieving Leaf Area Index (LAI) Using Remote Sensing: Theories, Methods and Sensors. *Sensors*, *9*, 2719–2745. doi:10.3390/s90402719 (open access).